Ultrafast Electronic Dynamics in Solid and Liquid Gallium Nanoparticles

M. Nisoli, S. Stagira, and S. De Silvestri
Centro di Elettronica Quantistica e Strumentazione Elettronica-CNR, Dipartimento di Fisica, Politecnico, Milano, Italy

A. Stella and P. Tognini
Istituto Nazionale per la Fisica della Materia-Dipartimento di Fisica "A. Volta," Università degli Studi, Pavia, Italy

P. Cheyssac and R. Kofman
Laboratoire de Physique de la Matière Condensée, URA 190, Université de Nice, Sophia Antipolis, Nice Cedex, France

(Received 26 December 1996)

The electron thermalization process both in solid and liquid metallic gallium nanoparticles with radii in the range 50–90 Å is investigated by femtosecond pump-probe measurements. The results show that the temporal behavior of the electron energy relaxation is similar in both phases, with a time constant varying from ~0.6 to ~1.6 ps by increasing the nanoparticle size. We interpret the experimental data in terms of a size-dependent electron-surface interaction model and show the importance of the energy exchange with surface phonons in the electronic thermalization. [S0031-9007(97)03100-1]

PACS numbers: 78.47.+p, 71.24.+q

The electron relaxation dynamics in metallic nanoparticles is the object of active experimental investigations [1–4]. Space confinement of the electronic wave function in metallic nanoparticles leads to relevant modifications of thermodynamic, electronic, and optical properties with respect to the bulk [5–7]. This constitutes the basis for new and important developments both in terms of fundamental properties and applications [8]. A typical signature of the optical response of metallic nanoparticles is given by the presence of the surface plasmon resonance whose linewidth depends on the interaction with the embedding matrix [9]. It should be noted that, being the plasmon linewidth determined by the phase-coherence time of the collective excitation, it cannot be directly related to the energy relaxation dynamics of the electron distribution. Previous transient pump-probe experiments were performed in order to investigate the electron relaxation dynamics in metallic nanoparticles in a dielectric matrix and the results were interpreted in terms of bulk electron-phonon and electron-electron interactions [1,3]. In a recent work the authors reported a size dependence of the electronic thermalization process in tin nanoparticles pointing out the role of electron-surface interaction [4].

In this work we adopted a novel experimental approach to investigate the different mechanisms leading to the electron thermalization in metallic nanoparticles; i.e., we performed femtosecond pump-probe measurements on gallium nanoparticles in both the liquid and solid phases: this in order to clarify the role of the lattice in the electron relaxation process. Gallium nanoparticles (with radii from 50 to 90 Å) are particularly suitable in this respect since they are liquid at room temperature and solid at liquid nitrogen temperature. We show that in sufficiently small metallic nanoparticles the dominant effect in electron-lattice energy exchange is the interaction between electrons and surface vibrational modes in both liquid and solid phases.

The samples were prepared by evaporation-condensation of high purity gallium in ultrahigh vacuum on sapphire substrates [4,10]. After evaporation of a thin film of SiO_x ($x \approx 1$), Ga was deposited. Metal particles were thus formed, which were subsequently covered and protected by an addition layer of SiO_x. This technique allows us to obtain nanoparticles in a wide size range and with a relatively low size dispersion (≤20%) and minimizes any strain or stress effects on the particles. The nanoparticle shape is that of a truncated sphere (from the contact angle Ga-SiO, the volume of the truncated spheres can be calculated to be more than 80% of that of ideally perfect spheres with the same radius). The measurements were performed on three gallium samples with radii of 50 (Ga1), 70 (Ga2), and 90 (Ga3) Å; the sizes of the nanoparticles have been obtained by transmission electron microscopy measurements. A typical optical spectrum is shown in Fig. 1, where the peak due to the surface-plasmon resonance is centered around 3 eV (~410 nm), where it is expected to fall according to the formula $\omega^* = \omega_p/\sqrt{1 + 2\varepsilon_r}$, ω_p being the gallium bulk plasma frequency (~10 eV [11]), and $\varepsilon_r \approx 4.4$ [12] the relative dielectric constant of the SiO matrix. The difference in the peak position of the plasma resonance between solid and liquid states is negligible. Similar results can be found in the reflectivity spectra of the samples.

Transient transmissivity and reflectivity measurements were performed by using a conventional pump-probe configuration. The laser system consists of a Ti:sapphire laser with chirped-pulse amplification, which provides pulses of 150-fs duration at 780 nm with energy up to 750 μJ at 1-kHz repetition rate. The experiments were performed at pump and probe wavelengths of 390 and

0031-9007/97/78(18)/3575(4)$10.00

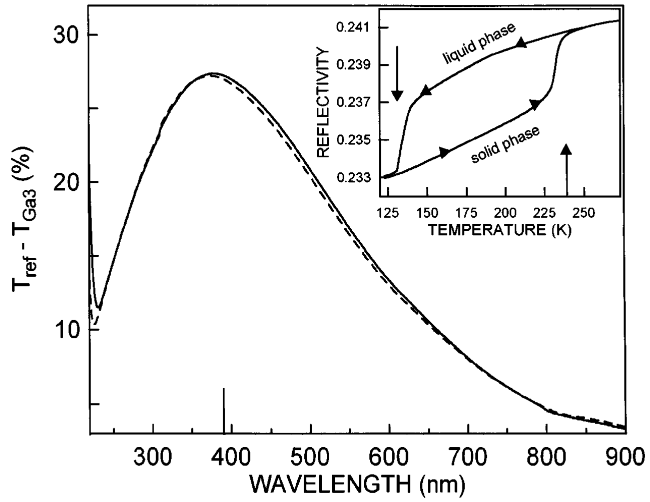

FIG. 1. Differential transmission of sample Ga3 with respect to a reference sample (without nanoparticles): $T \approx 77$ K (solid curve), $T \approx 300$ K (dashed curve). The mark indicates the pump pulse wavelength. The reflectivity hysteresis curve (measured at 632 nm) due to solid-liquid (↑) and liquid-solid (↓) transitions is shown in the inset.

780 nm, respectively. The 390-nm pump beam, which is resonant with the nanoparticle plasmon peak, was obtained by frequency doubling a fraction of the laser beam in a LiB_3O_5 crystal of 1-mm length. The excitation pulse duration was 180 fs and the energy used in the experiment was 37 nJ. The pump and probe beams were focused onto the sample to focal spots with diameter of ~240 and 100 μm, respectively.

The transient transmission changes ΔT in the three gallium samples at 77 K (solid phase) are shown in Fig. 2(a) as a function of probe time delay. The transient transmission curves show a rise time that follows the time integral of the pump-probe cross-correlation function and an initial fast decay which exhibits a clear size dependence. The time evolution of ΔT for Ga2 on an extended time scale is shown in Fig. 2(b); a similar time evolution was observed in the data measured for Ga1 and Ga3. The values of the time constant τ associated to the initial decay, obtained by best fitting of the experimental curves, are reported in Table I. Similar temporal behaviors were observed in transient reflectivity. By warming up the samples, the nanoparticles become liquid below room temperature as demonstrated by the reflectivity hysteresis curve shown in the inset of Fig. 1. The transient transmission changes ΔT measured for the three gallium samples at room temperature (liquid phase) follow temporal evolutions similar to those observed in the solid phase but with slightly longer time constants τ (see Table I).

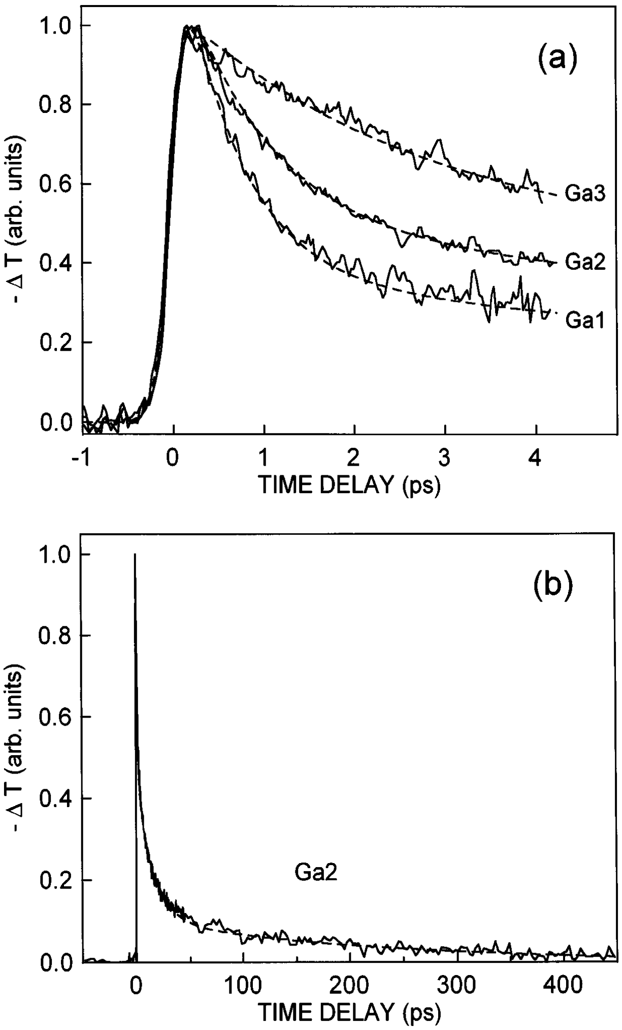

FIG. 2. (a) Transient transmissivity changes ΔT in Ga1, 2, and 3, as a function of probe time delay; the dashed lines are fitting curves; (b) ΔT in Ga2 on an extended time scale; the dashed line is the fitting curve (the sampling density has been increased for small time delay to show the actual time decay).

TABLE I. Time constants τ obtained from the fitting of the transient transmissivity curves for solid and liquid nanoparticles, and values of τ_{th} estimated by the model described in the text.

		Solid phase ($T = 77$ K)		Liquid phase ($T = 293$ K)	
Sample	Radius (Å)	τ (fs)	τ_{th} (fs)	τ (fs)	τ_{th} (fs)
Ga1	50	650 ± 30	630	750 ± 40	740
Ga2	70	1000 ± 50	1030	1200 ± 60	1180
Ga3	90	1500 ± 70	1450	1650 ± 80	1620

The electron relaxation dynamics in metallic nanoparticles is usually described by the electron-phonon coupling model developed for bulk metals [13–15]. We demonstrate here that in very small metallic nanoparticles the electron thermalization process is substantially different from that in bulk. In fact, if the radius R of the nanoparticle is comparable or smaller than the bulk electron mean free path, scattering of the electrons from the surface of the nanoparticle becomes relevant and the electrons oscillate inside the spherical potential well of the particle with a frequency $\nu = v_F/R$ [16,17], where v_F is the Fermi velocity. In sufficiently small particles this frequency can be larger than the Debye frequency, so that the bulk electron-phonon interaction (which is a resonant process) may become ineffective [17,18]. In this case the electrons dissipate the excess energy through generation of surface vibrational waves, defined as capillary waves [19]. In the case of gallium nanoparticles the mean free path at 77 K is ~150 Å [20,21], i.e., larger than the maximum radius of the nanoparticles studied in the present work. Therefore, the electron scattering with the surface takes place and the corresponding minimum charge oscillation frequency $\nu = 1.82 \times 10^{14}\ \mathrm{s}^{-1}$ ($v_F \sim 1.64 \times 10^6\ \mathrm{m\,s}^{-1}$ [21]) turns out to be much larger than the gallium Debye frequency $\nu_D = 6.6 \times 10^{12}\ \mathrm{s}^{-1}$ [20]. Interaction between electrons and surface modes thus plays a relevant role in the electron relaxation dynamics. The time constants τ reported in Table I are related to this process.

The time evolution of the electron and lattice effective temperatures, T_e and T_L, respectively, can be described by a set of two coupled differential equations [22,23]:

$$C_e(T_e)\frac{\partial T_e}{\partial t} = -\alpha(T_e - T_L) + P(t), \qquad (1)$$

$$C_L\frac{\partial T_L}{\partial t} = \alpha(T_e - T_L), \qquad (2)$$

where $C_e(T_e)$ and C_L are the electronic and lattice heat capacities per unit volume, α is a constant related to the electron-surface energy exchange, and $P(t)$ is the absorbed laser power density. In Eqs. (1) and (2) we treat the electron energy losses in the same way as in the bulk; i.e., we suppose them proportional to the difference between the electron and lattice temperatures, but considering a coupling constant α, which takes into account surface effects. The electron-surface phonon (e-sp) coupling constant in small metallic particles can be derived in the framework of a quantum-kinetic treatment [24]. The energy released per unit time by the hot electron population in the nanoparticle, given by $\partial E/\partial t = 4\pi\alpha(T_e - T_L)R^3/3$, can be expressed in terms of the microscopic parameters of the electron gas as follows [24]:

$$\frac{\partial E}{\partial t} = \sum_{\nu} \varepsilon_\nu \hat{I} f_{\nu\nu}, \qquad (3)$$

where ε_ν is the electron energy, $f_{\nu\nu}$ the occupation function of a given state, and $\hat{I}$ the electron-phonon collision integral. By considering the Hamiltonian which describes the interaction of electrons in a spherical potential well of depth V_0 with the capillary oscillations the following expression for the e-sp coupling constant α is obtained [24]:

$$\alpha = \frac{3}{16\pi} k_B \frac{v_F}{R} n \frac{m_e \omega_0^2}{\sigma}\left(\frac{V_0}{\varphi_0}\right)^2, \qquad (4)$$

where k_B is the Boltzmann constant, n the electron concentration, m_e the electron mass, σ the surface tension coefficient, ω_0 the maximum frequency of the surface modes, and φ_0 the work function. To calculate the frequencies of the surface modes each particle is assumed to be a perfectly spherical droplet with uniform density ρ [19,25]. The mode frequencies ω_l are determined by the boundary condition of the equation of motion for the velocity potential, which describes the hydrodynamics of the droplet [25]:

$$\frac{\rho\omega_l^2 R^2}{\sigma[l(l+1) - 2]} = \frac{l + 1/2}{R}\,\frac{J_{l-1/2}(\omega_l R s^{-1}) - J_{l+3/2}(\omega_l R s^{-1})}{J_{l-1/2}(\omega_l R s^{-1}) + J_{l+3/2}(\omega_l R s^{-1})} - \frac{1}{2R}, \qquad (5)$$

where s is the sound velocity and the J are Bessel functions. The maximum frequency ω_0 of the surface modes corresponds to the largest integer value l smaller than $\pi R/d$, with d the mean interatomic distance. Assuming the following parameters: $n = 15.4 \times 10^{28}\ \mathrm{m}^{-3}$, $\sigma \sim 0.36\ \mathrm{J\,m}^{-2}$, $\rho = 5.9 \times 10^3\ \mathrm{Kg\,m}^{-3}$, $s \sim 4.8 \times 10^3\ \mathrm{m\,s}^{-1}$, $\varphi_0 = 3.96$ eV, $V_0 = 10.71$ eV, and $d = 2.9$ Å [20,21,26,27], and using Eqs. (4) and (5) we obtain for α the values reported in Table II. It should be noted that the e-sp coupling constant α is of the same order of magnitude of the e-p coupling constant of bulk metals [1,3]. By using the calculated values of α in the coupled differential equations (1) and (2) it is possible to calculate the time evolution of the effective electron and lattice temperatures after laser excitation. The parameters used are $C_e(T_e) = \gamma T_e$ with $\gamma = 50.8\ \mathrm{J\,m}^{-3}\,\mathrm{K}^{-2}$ [20], and $C_L = 1.31 \times 10^6\ \mathrm{J\,m}^{-3}\,\mathrm{K}^{-1}$ at 77 K [27]. We define as time constant τ_{th} of the temperature evolution the time required to decay to $1/e$ of the peak value. For the induced temperature changes in our experiment, the transient transmissivity can be considered proportional to the electron temperature variations. The time constants τ_{th}, reported in Table I, turn out to be in good agreement with those measured from the transient transmission curves. Therefore the observed size dependence of the electron relaxation process can be entirely ascribed to the size dependence of the e-sp coupling constant α.

TABLE II. Calculated values of the electron-surface phonon coupling constant α.

Sample	α ($\times 10^{16}$ W m^{-3} K^{-1})
Ga1	5.928
Ga2	4.114
Ga3	3.248

The similarity in the electron relaxation dynamics observed in solid and liquid nanoparticles cannot be explained in the framework of the bulk e-p coupling model. In fact the bulk electron energy loss mechanisms are substantially different in the two phases, while our experimental results show an electron thermalization dynamics almost independent of the phase. Within the e-sp coupling model the observed small difference in the time constant in solid and liquid nanoparticles is explained by the different heat capacities C_L (2.48×10^6 [27] and 1.31×10^6 J m^{-3} K^{-1}, at 293 and 77 K, respectively). The calculated time constant τ_{th} reported in Table I are again in good agreement with the measured ones.

In conclusion, we have studied the ultrafast electron dynamics in gallium nanoparticles of different sizes in the solid and liquid phase. The results show that the temporal behavior of the electron energy relaxation is similar in both phases, with clear size-dependent characteristic time constants. The experimental data have been interpreted in terms of an electron-surface interaction model, with no need of introducing additional effects of any kind from the matrix on the thermalization process. These results bring new information on the role of the energy exchange with surface phonons in the electronic thermalization process occurring in confined metallic structures.

This work was partially supported by Consiglio Nazionale delle Ricerche and Istituto Nazionale per la Fisica della Materia.

[1] T. Tokizaki, A. Nakamura, S. Kaneko, K. Uchida, S. Omi, H. Tanji, and Y. Asahara, Appl. Phys. Lett. **65**, 941 (1994).

[2] T. W. Roberti, B. A. Smith, and J. Z. Zhang, J. Chem. Phys. **102**, 3860 (1995).

[3] J. Y. Bigot, J. C. Merle, O. Cregut, and A. Daunois, Phys. Rev. Lett. **75**, 4702 (1995).

[4] A. Stella, M. Nisoli, S. De Silvestri, O. Svelto, G. Lanzani, P. Cheyssac, and R. Kofman, Phys. Rev. B **53**, 15 497 (1996).

[5] J. A. Perenboom, P. Wyder, and M. Meier, Phys. Rep. **78**, 173 (1981).

[6] W. P. Halperin, Rev. Mod. Phys. **58**, 533 (1986).

[7] C. Flytzanis, F. Hache, M. C. Klein, D. Ricard, and P. Roussignol, in *Progress in Optics XXIX*, edited by E. Wolf (Elsevier, Amsterdam, 1991), p. 321.

[8] R. S. Service, Science **271**, 920 (1996); C. B. Murray, C. R. Kagan, and M. G. Bawendi, Science **270**, 1335 (1996).

[9] H. Hövel, S. Fritz, A. Hilger, U. Kreibig, and M. Vollmer, Phys. Rev. B **48**, 18 178 (1993).

[10] E. Sondergard, R. Kofman, P. Cheyssac, and A. Stella, Surf. Sci. **364**, 467 (1996).

[11] R. Kofman, P. Cheyssac, and J. Richard, Phys. Rev. B **16**, 5216 (1977).

[12] H. R. Philipp, in *Handbook of Optical Constants of Solids*, edited by E. D. Palik (Academic, New York, 1985).

[13] H. E. Elsayed-Ali, T. B. Norris, M. A. Pessot, and G. A. Mourou, Phys. Rev. Lett. **58**, 1212 (1987).

[14] R. W. Schoenlein, W. Z. Lin, J. G. Fujimoto, and G. L. Eesley, Phys. Rev. Lett. **58**, 1680 (1987).

[15] C.-K. Sun, F. Vallée, L. Acioli, E. P. Ippen, and J. G. Fujimoto, Phys. Rev. B **48**, 12 365 (1993).

[16] U. Kreibig and C. V. Fragstein, Z. Phys. **224**, 307 (1969).

[17] E. D. Belotskii and P. M. Tomchuk, Surf. Sci. **239**, 143 (1990).

[18] S. A. Gorban', S. A. Nepijko, and P. M. Tomchuk, Int. J. Electron. **70**, 485 (1991).

[19] L. D. Landau and E. M. Lifshitz, *Fluid Mechanics* (Pergamon, Oxford, 1982).

[20] *American Institute of Physics Handbook* (McGraw-Hill, New York, 1972), 3rd ed.

[21] D. A. Papaconstantopoulos, *Handbook of the Band Structure of Elemental Solids* (Plenum, New York, 1986).

[22] S. I. Anisimov, B. L. Kapeliovich, and T. L. Perel'man, Sov. Phys. JETP **39**, 375 (1974).

[23] G. L. Eesley, Phys. Rev. B **33**, 2144 (1986).

[24] E. D. Belotskii and P. M. Tomchuk, Int. J. Electron. **73**, 955 (1992).

[25] V. M. Akulin, E. Borsella, and A. A. Nesterenko, Phys. Rev. Lett. **73**, 1231 (1994).

[26] N. W. Ashcroft and N. D. Mermin, *Solid State Physics* (Holt-Saunders, Orlando, 1976).

[27] P. de la Breteque, *Gallium* (Alusuisse, Geneva, 1970).